

Compensation for Biodynamic Feedthrough in Backhoe Operation by Cab Vibration Control

Heather C. Humphreys, Dr. Wayne J. Book and James D. Huggins, *Members, IEEE*

Abstract—This research investigates and seeks to mitigate the undesirable effects of biodynamic feedthrough in backhoe operation. Biodynamic feedthrough occurs when motion of the controlled machine excites motion of the human operator, which is fed back into the control input device. This unwanted input can cause significant performance degradation, which can include limit cycles or even instability. Backhoe user interface designers indicate that this is a problem in many conventional machines, and it has also proved to degrade performance in this testbed. A particular backhoe control system, including the biodynamic feedthrough, is modeled and simulated. Cab vibration control is selected as a means to mitigate the biodynamic feedthrough effect. Two controller based methods are developed based on these models and presented, both of which use the working implement itself to reduce the cab motion. In this case, the backhoe arm has dual functionality, to perform excavation operations and to cancel cab vibration. Results show that significant reductions in cab motion can be obtained with minimal tracking performance degradation, without additional actuators.

I. INTRODUCTION

BIODYNAMIC FEEDTHROUGH is a widely recognized problem in operation of backhoes and excavators. This phenomenon occurs when motion of the controlled machine excites motion of the human operator, which is fed back into the control device. This unwanted input causes significant performance degradation, which can include limit cycles or even instability. It cannot be measured during operation, since it cannot be decoupled from the operator's desired command. It is correlated with the output and acts as a feedback loop, which can go unstable under some circumstances. The main goals of this research are to investigate and model the effect of biodynamic feedthrough on a backhoe control system and to develop compensation to reduce the adverse effects.

Several methods have been considered for biodynamic feedthrough compensation in a variety of systems. One common approach is to subtract away an estimate of the feedthrough-induced component of the operator input. This can be achieved by measuring the cab motion and estimating

the undesirable signal component from a model of the human operator; however, the human operator is highly variable and difficult to model accurately. Another approach is to minimize the cab vibration, which subsequently reduces the human body excitation. Cab vibration reduction can be obtained by a variety of methods, including vibration isolation, filtering or command shaping, active vibration control using additional actuators, or active vibration control using the working implement itself. Controller-based methods which do not require additional hardware are attractive since they do not add significant cost to the machine; cost is a significant limiting factor in the mobile hydraulics industry. This research focuses on compensation for biodynamic feedthrough by reduction of cab vibration. This work presents a first step toward solving the complex problem of biodynamic feedthrough.

II. BACKGROUND

A. *Haptically Enhanced Robotic Excavator (HENRE)*

While the industry standard in backhoe control has remained as the same 2-joystick, 4-DOF mapping for several decades, several researchers have investigated the use of coordinated control. An advanced user interface for a backhoe has been developed at Georgia Tech, called the Haptically Enhanced Robotic Excavator (HENRE), which uses coordinated position control with haptic feedback. The HENRE system is described in [1], [2], [3], [4] and [5], and it is pictured in Fig. 1.

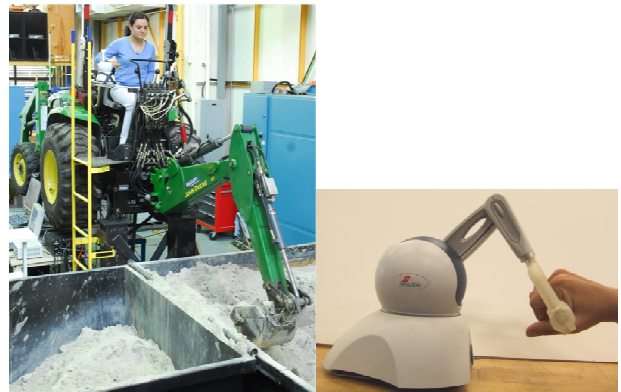


Fig. 1 HENRE Testbed and SensAble Omni input device

Manuscript received September 15, 2010. This work was supported in part by the U.S. Department of Defense through an NDSEG fellowship and by the John Deere Foundation.

H. C. Humphreys is with the Georgia Institute of Technology, Atlanta, GA 30332, USA (phone: 404-385-1883; e-mail: heather.humphreys@gatech.edu).

W. J. Book is with the Georgia Institute of Technology, Atlanta, GA 30332, USA (e-mail: wayne.book@me.gatech.edu).

J. D. Huggins is with the Georgia Institute of Technology, Atlanta, GA 30332, USA (e-mail: james.huggins@me.gatech.edu).

The HENRE system uses a SensAble Omni™ commercial six degree-of-freedom (DOF) haptic display input device

mounted beside the tractor seat. It enables coordinated position-to-position mapping from the input device to the backhoe arm. In contrast, conventional backhoe user interfaces use position-to-velocity mapping with two separate 2-DOF joysticks. Tests indicate that the coordinated control interface used on HEnRE provides more intuitive operation.

The system uses a 4410 series John Deere tractor with a Model 47 backhoe. It has been retrofitted with electro-hydraulic proportional directional valves, and it uses the original constant displacement pump. The system includes a wide array of sensors, including position sensors for each cylinder and a 3-axis MEMS accelerometer mounted on the base of the tractor seat.

The backhoe controller uses software written using MATLAB/Simulink™ with xPC Target™ for real-time control implemented on a dedicated PC-104 target. A separate Windows host PC is used for control of the SensAble Omni™. Communications are via Ethernet with UDP protocol, and the target sample rate is set to 1000 Hz.

B. Biodynamic Feedthrough

Biodynamic feedthrough is a widely recognized problem in the area of high-performance aircraft, and it has been an area of research in the aerospace industry for several decades. It is also significant in control of mobile hydraulic equipment, though it has received less attention in this area. The new electronic joysticks have more problems with biodynamic feedthrough than the earlier manual joysticks, as a result of less damping and smaller workspaces.

Only a few publications on biodynamic feedthrough consider hydraulic equipment applications. In [6], an investigation on biodynamic feedthrough in excavator operation is performed using simplified mass-spring-damper models, though the experimental validation of the modeling is limited.

An in-depth study on biodynamic feedthrough was performed by Systems Technology, Inc., under a contract for the US Air Force [7], [8]. It focuses on development of biomechanical models for the human pilot, to simulate the interaction between human body dynamics and structural modes in manual control systems. They assumed a pilot body position which makes the models invalid for the backhoe. In general, results indicate that biodynamic feedthrough effects are primarily of involuntary nature; any cognitive or neuro-muscular compensation is negligible. Two other investigations involve model-based cancellation for biodynamic feedthrough, based on experiments with a seated operator controlling a single degree-of-freedom platform; human variability is a significant problem in these approaches ([9], [10]). One patent describes an actuated “biodynamic resistant control stick” developed for aircraft control, which actively varies the joystick’s spring return force as a function of the aircraft motion [11].

Two publications present preliminary studies on biodynamic feedthrough in the HEnRE system. The first paper is focused solely on system modeling using the stick

joint; it presents development of a model showing the effects of the biodynamic feedthrough, with subsystem models for each of the major dynamic components, including the human body, with parameters specific to the HEnRE hardware [12]. A second paper provides an overview of the problem and presents ideas for a few controller-based approaches for reducing cab acceleration, along with some simulation results ([13], [14]). This paper focuses on the controller development, utilizing the boom joint, providing a detailed description of several controller designs and results from hardware testing.

C. Active Control of Cab Vibration

Numerous publications over past decades involve active vibration control designs for minimization of cab motion in vehicles, primarily for ergonomic purposes. For example, one simulation study uses a sky-hook damping approach, using a linear quadratic regulator (LQR) optimal controller, with actuated suspension for vibration control of a quarter car model [15]. Rahmfeld and Ivantysynova present a review paper that discusses various forms of passive, semi-active and active vibration control for mobile hydraulic equipment structures [16]. In [17], active cab motion reduction for a wheel loader is achieved using an LQR-based state feedback controller. The working implement has dual functionality, but it serves each purpose at different times during operation.

III. APPROACH

A controller based approach is proposed, using the working implement for simultaneous dual functionality, both for excavation tasks and for cab vibration reduction. This vibration reduction could be achieved by several active or passive methods, such as filtering, input shaping or various forms of active vibration control. In all such cases, the controller has conflicting objectives, and the tradeoff between working performance and cab vibration reduction must be addressed.

The process of designing this controller involves several steps: modeling, controller design and simulation, and experimental validation. These are the focus of this paper. Biodynamic feedthrough presents a very complex problem in the control of high degree-of-freedom machines such as backhoes and excavators. As an initial step, some significant simplifications and assumptions were made.

The system is limited to a single degree-of-freedom, fore-aft motion with small motions of the arm. This approximation is made possible by operating the backhoe only within a small angle approximation and in an approximately vertical configuration, producing primarily fore-aft motion of the backhoe arm, the cab, and the human body. This backhoe configuration was selected in order to maximize cab vibration excitation while providing single degree of freedom (DOF) excitation of the cab. Expanding the solution to multiple degrees of freedom is a key subject for future work.

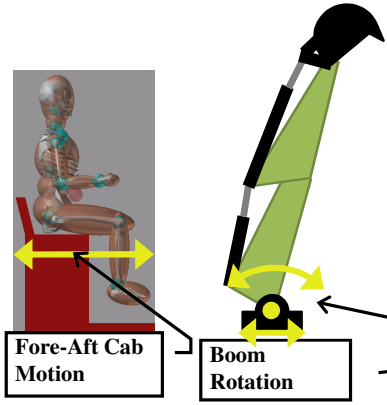


Fig. 2 Rotation of the boom link within a small angle approximation produces primarily fore-aft excitation of the cab.

IV. MODELING

The main dynamic components of the system were modeled using a hybrid of first principles and system identification. General forms of linear equations were assumed based on first principles, and parameters were determined from frequency domain system identification. A detailed description of the modeling of this system is given in [12].

The transfer function from valve command signal $V(s)$ to cylinder position $Y(s)$ is given by the following equation.

$$\frac{Y(s)}{V(s)} = \frac{K_{vc}}{s} \cdot \frac{\omega_{nvc}^2}{s^2 + 2\zeta_{vc}\omega_{nvc}s + \omega_{nvc}^2} \quad (1)$$

The term K_{vc} denotes the gain, ζ_{vc} is the damping coefficient, and ω_{vc} denotes natural frequency. The model includes the integration term from valve command to cylinder position, as well as a term for heavily damped second order dynamics. The corresponding frequency response, or Bode magnitude plot, is shown in Fig. 3.

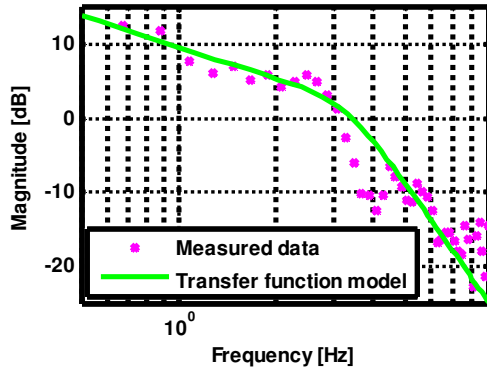


Fig. 3 Valve/Cylinder frequency response magnitude plot, measurement and model

Similarly, the transfer function from the cylinder position $Y(s)$ to the cab position $C(s)$ is given by the following.

$$\frac{C(s)}{Y(s)} = K_s \cdot \frac{2\zeta_{s1}\omega_{ns1}s + \omega_{ns1}^2}{s^2 + 2\zeta_{ns1}\omega_{ns1}s + \omega_{ns1}^2} \cdot \frac{2\zeta_{ns2}\omega_{ns2}s + \omega_{ns2}^2}{s^2 + 2\zeta_{ns2}\omega_{ns2}s + \omega_{ns2}^2} \quad (2)$$

This model is based on a 2-mass-spring-damper system; the frequency response of the structure has two clear peaks in the frequency range of interest. The system identification is based on measurements of cylinder position and cab acceleration, also resulting from a swept sine valve excitation. Fig. 4 shows the corresponding frequency response magnitude plot, from cylinder position to seat acceleration. The model and measured data match well except for very low frequencies. At low frequencies, the cab vibration amplitude is very low, and the coherence is low. The small mismatch between the data and model at low frequencies has little effect on biodynamic feedthrough compensation development, since only minimal cab and human excitation occurs at low frequencies.

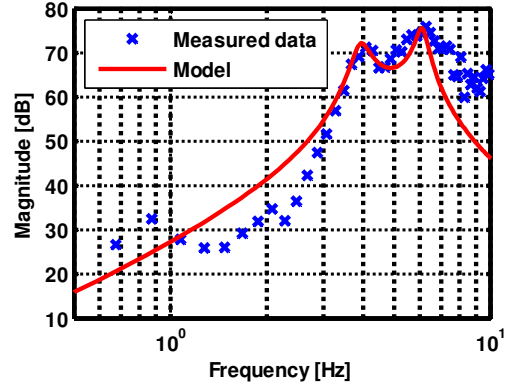


Fig. 4 Structure frequency response magnitude plot, measurement and model

Model parameters for the structure and valve/cylinder subsystems are given in Table 1. These parameters were used for the design of the controllers. The human body model was used only for simulation of the dynamic system with biodynamic feedthrough, not for controller design. This is desirable, since the biomechanical model parameters are expected to vary widely.

TABLE I
MODEL PARAMETER VALUES

Model Parameter	Numerical Value
K_{vc}	22.0
ω_{nvc} [Hz]	3.37
ζ_{vc}	0.45
K_s	0.45
ω_{ns1} [Hz]	4.0
ζ_{s1}	0.06
ω_{ns2} [Hz]	6.2
ζ_{s2}	0.04

The human body biomechanics present a very complex dynamic system. In order to simplify the model, the human body was considered only in approximately the kinematic configuration of a seated operator. System identification was used to determine the simplest model that captures the dominant dynamics in the system operating frequency range. Two different approaches were taken to determine the measurements. First, the input-output relationship was determined by human experiments. Second, the LifeMOD human body biodynamics modeling add-on to MSC.Adams was used to simulate the same experiment, with excitation of the seat and recording of hand motion. The data did show considerable variation, as expected. The simplest model that approximates the response of the expected range of human biomechanics is most appropriate, rather than a detailed model that matches one human parameter set very closely. The model form that best matched the range of human body mechanics data assumed the body to be only a mass, neglecting the dynamics. Therefore, the transfer function from the cab position $C(s)$ to the resulting hand position $H(s)$ can be modeled simply as a gain, K_H . A more detailed description of the human body modeling is given in [12].

V. CLASSICAL CONTROL TECHNIQUES

Several different forms of classical and state-space controllers were developed and simulated in MATLAB/Simulink™ and tested in hardware, starting with the simplest and progressing to more complex. The goals for these controllers are to achieve adequate cylinder tracking performance while minimizing cab motion excitation. Two are presented in this paper, (1) a simple PID cylinder controller with a notch filter at the structure natural frequency and (2) an active damping approach. Fig. 6 shows a block diagram of the classical control system with the notch filter, including the inner cylinder control loop and the outer biodynamic feedthrough loop. The standard form of the PID controller is used.

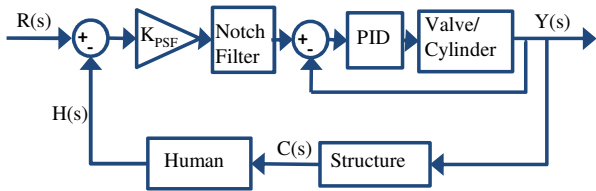


Fig. 5 Classical block diagram for cylinder position control, including biodynamic feedthrough

Equation 4 gives the transfer function for the notch filter.

$$D_{nf} = \frac{s^2 + 2\zeta_{nf}\omega_{nf}s + \omega_{nf}^2}{(s + \omega_{nf})^2} \quad (4)$$

The zeros of the filter are placed at a frequency midway between the two distinct natural frequencies of the structure, and the damping is tuned such that the desired magnitude

reduction is obtained at both natural frequency peaks. Note that the filter is inside the biodynamic feedthrough loop but outside the valve feedback control loop. In this system, the outer loop closed loop pole locations are very close to the open loop pole locations. Therefore, it is reasonable to design the notch filter primarily based on open-outer-loop performance.

The notch filter has the advantage of simplicity, but it does not utilize the measured cab vibration as feedback, so it does not provide disturbance rejection or compensate for any unmodeled cab motion.

VI. FULL-STATE FEEDBACK CONTROL TECHNIQUES

Another control strategy for cab vibration reduction actively utilizes the measured cab acceleration as feedback to reduce cab vibration. This approach is implemented as a full state feedback optimal Linear Quadratic Regulator (LQR). This has the advantage of providing some disturbance rejection and compensation for unmodeled structural vibrations.

The valve/cylinder response in this structural configuration has significant nonlinear effects, resulting from unequal piston-side and rod-side pressures, gravitational effects, cylinder stiction, valve deadband and saturation, and others. An inner proportional-only cylinder velocity control loop was added in order to improve the linearity of response. The state feedback control is applied external to this velocity-controlled cylinder. The inner loop also serves to speed up the valve response slightly, such that the valve response is sufficiently fast relative to the structure dynamics. Only cylinder position is measured; therefore, the cylinder measurement must be differentiated to give the cylinder velocity feedback. The position measurement proves to be sufficiently smooth that this differentiation, after low-pass filtering, provides meaningful feedback. Fig. 6 shows this inner velocity feedback loop.

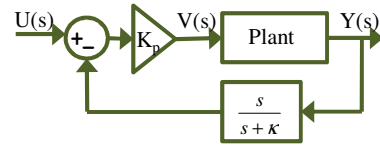


Fig. 6 Inner cylinder velocity feedback loop

The closed loop transfer function for the valve/cylinder dynamics with proportional velocity feedback is given in Eqn. 5.

$$\frac{Y(s)}{U(s)} = \frac{K_P K_{vc} \omega_{nvc}^2}{s(s^2 + 2\zeta_{vc}\omega_{nvc}s + \omega_{nvc}^2 + K_P K_{vc} \omega_{nvc}^2)} \quad (5)$$

This valve/cylinder model with proportional velocity control (Eqn. 5) is combined with the structural dynamics model (Eqn. 2) to produce a single-input, two-output state space system.

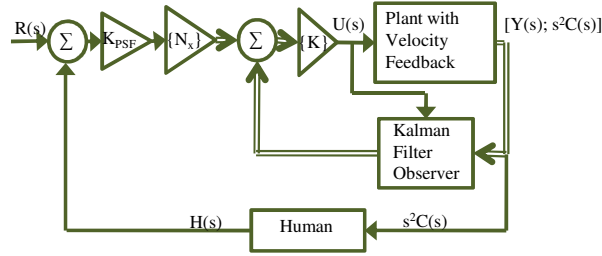


Fig. 7 Full state feedback block diagram

The input to this system is the reference cylinder position $R(s)$, and the measurements are cylinder position $Y(s)$ and cab acceleration ($s^2 \cdot C(s)$). The human body biodynamics are not included in this state space system, since this part of the system cannot be controlled. By minimizing cab motion, the controller minimizes the input to the human body biodynamics.

The controller has two conflicting objectives, to reduce cab motion and drive cylinder position to a reference. This makes the LQR optimal control method a suitable choice for selecting the state feedback gains. This method allows the designer to choose weights to vary the tradeoffs between control effort and performance, as well as the tradeoffs between individual states.

A number of variations on this LQR controller were tested both in hardware and simulation. The best results were achieved from an active vibration damping approach. Active damping is obtained by feeding back cab velocity rather than cab acceleration; this is obtained by integrating the measured cab acceleration signal in real time. This integration also has a smoothing effect on the noisy acceleration measurement.

The cost function for the LQR optimization is given by

$$J = \int_0^\infty (x^T Q_{LQR} x + u^T R_{LQR} u) dt \quad (6)$$

where x the state vector, u is the control signal, and Q_{LQR} and R_{LQR} are weighting matrices. The relative values between Q_{LQR} and R_{LQR} determine the tradeoff between performance and control effort, while the values within the Q_{LQR} matrix determine the tradeoff between the states. In order to apply weights to the individual outputs rather than individual states, we use an additional weighting matrix Y , as shown in Eqn. 7.

$$Y = \begin{bmatrix} \alpha & 0 \\ 0 & \beta \end{bmatrix} \quad (7)$$

The term α is a weight for the cylinder position output, and the term β is a weight for the cab velocity output. This matrix and the output matrix C are used to determine Q_{LQR} .

$$Q_{LQR} = [(Y \cdot C)^T (Y \cdot C)], \quad R_{LQR} = 1 \quad (8)$$

From this LQR optimization, the optimal feedback gain

matrix K is determined based on the well-known matrix Ricatti equation, or by the $lqr(*)$ function in MATLAB. The terms α and β were optimized by a coarse pattern search, by testing the controller on the hardware for each possible combination of gains.

The \bar{N} method described in [18] is used to introduce the cylinder position reference signal. In this case, the reference term added to control effort N_u is zero, and the reference multiplied by N_x is added to the states.

$$\begin{bmatrix} N_x \\ N_u \end{bmatrix} = \begin{bmatrix} A & B \\ C & D \end{bmatrix}^{-1} \cdot \begin{bmatrix} 0 \\ 1 \end{bmatrix}, \quad N_u = 0 \quad (9)$$

The system is represented in state space form by the standard convention of A , B , C and D matrices. The system has 7 states, with only two measurable, so an observer is needed; a full state observer was selected. The acceleration measurement is inherently noisy, so the Kalman filter is a suitable choice for determining optimal observer gains L_k to appropriately filter the measurements. This observer requires discretization of the system.

For the Kalman filter development, reasonable estimates of the process noise and measurement noise are needed. The measurement noise covariance matrix R_k was determined experimentally. Measurements of both system outputs, cylinder position and cab velocity (integrated cab acceleration) were measured over time with zero excitation. The covariances were computed from these measurements and used to compute R_k . The process noise levels are less well known. In order to estimate these levels, the approximate signal range for each state was determined from simulation. The process noise levels were assumed to be 5% of the signal range for each state. These were used to estimate a process noise covariance matrix Q_k .

The iterative calculation of the Kalman filter gains was performed offline, using the following standard iterative equations. Each iteration includes two steps; the innovation step is given by Eqn. 10, and the prediction step is given by Eqn. 11 and Eqn. 12.

$$P_k = P_k^- - L_k C_d P_k^- \quad (10)$$

$$P_{k+1} = \Phi P_k \Phi^T + G Q_k G^T \quad (11)$$

$$L_{(k+1)} = P_{k+1} C_d^T (C_d P_{k+1} C_d^T + R_k)^{-1} \quad (12)$$

The terms Q_k and R_k are the covariance matrices, the terms Φ and C_d are the discrete state transition and output matrices, and the term P_k is an intermediate term. The observer gain matrix L converges to the optimal gains.

VII. HARDWARE TEST RESULTS

Two different types of experiments are proposed to validate these controller designs, one with the human in the loop and one without.

1) Using a software input, with no human in the loop, test

tracking performance and cab vibration reduction with and without biodynamic feedthrough compensation.

- 2) Perform human in the loop experiments, comparing performance with the operator on and off the tractor.

The hardware experiments without the human in the loop were performed, and results are presented.

A. Classical Control with Notch Filter

Measured results for cylinder tracking and cab acceleration were obtained for two different inputs, a trapezoidal velocity profile and a swept sine.

Fig. 8 shows the trapezoidal tracking response for a PID controller with and without the notch filter. This response shows that the filter produces little performance degradation.

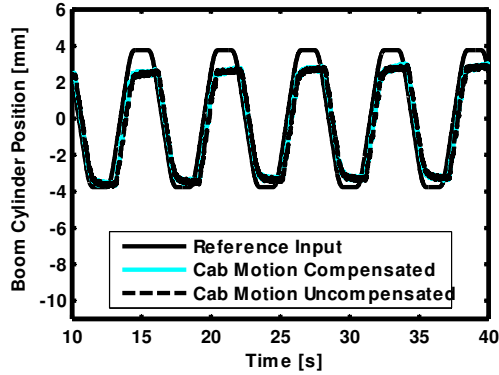


Fig. 8 Trapezoidal cylinder tracking with PID control, with and without notch filter

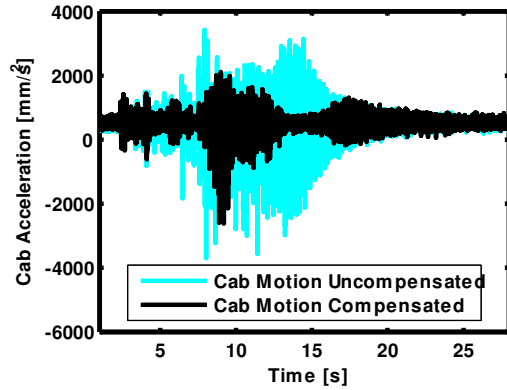


Fig. 9 Measured cab acceleration with PID control, with and without notch filter

Fig. 9 shows the measured cab accelerations resulting from a swept sine input to the valve. For the swept sine input, the *notch filter results in a 44% decrease in mean squared cab acceleration*, as compared with the same control architecture without the notch filter.

B. Full State Feedback Control

Similar sinusoidal and trapezoidal inputs were applied to the system with the LQR full state feedback control, and the experiments were performed with and without compensation for cab motion. The case without cab motion compensation

is obtained by setting the weight on the cab velocity term β in the Q_{LQR} matrix to zero; this results in zero controller gains applied to the cab motion states.

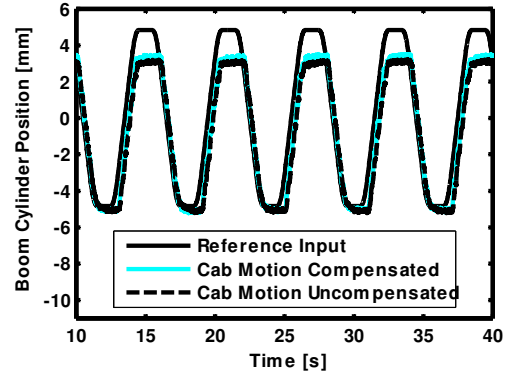


Fig. 10 Trapezoidal cylinder tracking with LQR control, with $\beta=0$ (no biodynamic feedthrough compensation) and $\beta=2$ (with biodynamic feedthrough compensation)

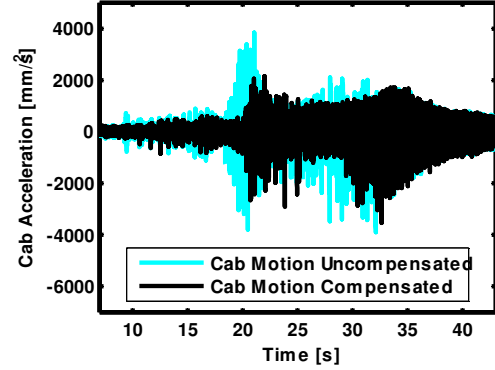


Fig. 11 Measured cab acceleration from swept sine excitation, with $\beta=0$ (no biodynamic feedthrough compensation) and $\beta=2$ (with biodynamic feedthrough compensation)

The trapezoidal cylinder tracking performance of the LQR controller is shown in Fig. 10. Similarly, Fig. 11 shows the cab vibration resulting from a swept sine input. With the swept sine input, the *LQR controller produces a 27% decrease in mean squared cab acceleration*, as compared with the same architecture without vibration compensation. Table 2 gives a summary of the results with the swept sine input.

TABLE II
MEAN SQUARED OUTPUT ERRORS FOR FOUR CONTROLLERS

Controller	Mean Squared Cab Acceleration [mm/s ² × 10 ⁵]	Mean Squared Tracking Error [mm]
PID – No Notch Filter	8.32	2.67
PID Plus Notch Filter	4.67	2.51
LQR, $\beta=0$	4.02	4.75
LQR, $\beta=2$	2.94	4.80

VIII. FUTURE WORK

Several additional steps are needed before these methods for biodynamic feedthrough compensation can be applied in industry. First, human subject tests are needed to validate the improvement in tracking performance. These tests will involve a comparison of operator tracking performance while seated on the tractor and on the ground beside the tractor. These tests are in progress.

A few other steps are also needed. One is to expand the control solutions to work in multiple degrees of freedom and address the complexities introduced by the kinematics of the machine. Another is to thoroughly investigate the robustness to a range of parameter variations, including structural variations, human operator variability, variations in loading conditions, and others. In addition, the tradeoff between control performance and vibration reduction merits further analysis, particularly in terms of determining what are the necessary performance criteria, in terms of bandwidth, damping and other specifications, which limit the allowable reduction in cylinder control performance.

IX. CONCLUSION

Experiments have demonstrated two types of control strategies that are able to significantly reduce cab vibration with minimal cylinder tracking performance degradation. This reduction in cab vibration subsequently reduces excitation of the human body, which is expected to reduce the unwanted input resulting from biodynamic feedthrough. Human subject tests are needed to validate the improvement in control performance resulting from this reduction in biodynamic feedthrough.

ACKNOWLEDGMENT

The authors thank LifeModeler for their contribution of the LifeMOD™ software.

REFERENCES

- [1] M. E. Kontz, "Haptic Control of Hydraulic Machinery Using Proportional Valves," PhD, Mechanical Engineering, Georgia Tech, Atlanta, GA, 2007.
- [2] M. E. Kontz, *et al.*, "Impedance shaping for improved feel in hydraulic systems," in *ASME Intl. Mech. Engr. Congr. Expo.*, Seattle, WA, 2007.
- [3] M. E. Kontz and W. J. Book, "Haptic enhancement of hydraulic equipment," in *FPNI-PhD Symposium*, Sarasota, FL, 2006, pp. 497-506.
- [4] M. E. Kontz and W. J. Book, "Electronic control of pump pressure for a small haptic backhoe," *Intl. Journal of Fluid Power*, vol. 8, Aug. 2007 2007.
- [5] M. E. Kontz and W. J. Book, "Flow Control for Coordinated Motion and Haptic Feedback," *Intl. Journal of Fluid Power*, vol. 8, pp. 5-16, Aug. 2007 2007.
- [6] F. Arai, *et al.*, "Dynamical Analysis and Suppression of Human Hunting in the Excavator Operation," in *IEEE Intl. Workshop on Robot and Human Interactive Communication*, Osaka, Japan, 2000, pp. 394-399.
- [7] R. W. Allen, *et al.*, "Manual Control Performance and Dynamic Response During Sinusoidal Vibration," Hawthorne, CA AMRL-TR-73-78, STI-TR-1013-2, 1973.
- [8] H. R. Jex and R. E. Magdaleno, "Biomechanical Models for Vibration Feedthrough to Hands and Head for a Semisupine Pilot," *Aviation, Space and Environmental Medicine*, vol. 49, pp. 304-316, 1978.
- [9] S. Sovenyi and R. B. Gillespie, "Cancellation of Biodynamic Feedthrough in Vehicle Control Tasks," *IEEE Transactions on Control Systems Technology*, vol. 15, pp. 1018-1029, Nov. 2007 2007.
- [10] M. R. Sirouspour and S. E. Salcudean, "Suppressing Operator-Induced Oscillations in Manual Control Systems with Moveable Bases," *IEEE Transactions on Control Systems Technology*, vol. 11, pp. 448-459, July 2003 2003.
- [11] D. W. Repperger, "Biodynamic Resistant Control Stick," vol. 4,477,043, S. o. t. U. S. A. Force, Ed., ed. United States: Secretary of the U.S. Air Force, 1984.
- [12] H. C. Humphreys, *et al.*, "Modeling of biodynamic feedthrough in backhoe operation," in *ASME Dynamic Systems and Control Conference*, Hollywood, CA, 2009.
- [13] H. C. Humphreys and W. J. Book, "Possible Methods for Biodynamic Feedthrough Compensation in Backhoe Operation," in *Fluid Power Net International 6th Annual PhD Symposium*, West Lafayette, IN, 2010.
- [14] H. C. Humphreys, "Modeling and Compensation for Biodynamic Feedthrough in Backhoe Operation," MS, Mechanical Engineering, Georgia Institute of Technology, Atlanta, 2010.
- [15] L. V. V. Gopala Rao and S. Narayanan, "Sky-hook control of nonlinear quarter car model traversing rough road matching performance of LQR control," *Journal of Sound and Vibration*, vol. 323, pp. 515-529, 2009.
- [16] R. Rahmfeld and M. Ivantysynova, "An overview about active oscillation damping of mobile machine structure," *Intl. Journal of Fluid Power*, vol. 5, pp. 5-24, 2004.
- [17] C. Williamson, *et al.*, "Active vibration damping for an off-road vehicle with displacement controlled actuators," *Intl. Journal of Fluid Power*, vol. 10, pp. 5-16, 2009.
- [18] C. Franklin and J. Powell, *Feedback Control of Dynamic Systems*, 1987.